# IMPROVING THE SIGNIFICANCE OF MM/SD RISK ANALYSIS BY APPLICATION OF THE SRL BALLISTIC LIMIT EQUATION

**Frank Schäfer(1), Robin Putzar(1), Shannon Ryan(2), Michel Lambert(3)**

(1)*Fraunhofer Institute for High-Speed Dynamics, Ernst-Mach-Institute, Eckerstr. 4, 79104 Freiburg, Germany, Email: frank.schaefer@emi.fraunhofer.de*
(2)*USRA Lunar and Planetary Institute, 3600 Bay Area Blvd, Houston, TX, 77058, USA*
(3)*ESA-ESTEC, Keplerlaan 1, 2201 AZ Noordwijk, The Netherlands*

## ABSTRACT

In this paper, a new ballistic limit equation (BLE) for satellite equipment placed behind satellite structure walls is presented. Application of this equation in micrometeoroid and space debris (MM/SD) risk analysis (RA) tools for satellites can lead to a more realistic quantitative assessment of the actual failure risk of satellite equipment from hypervelocity impacts (HVI) and hence, of the failure risk of a satellite. This is because in contrast to the BLEs that are currently in use in RA tools, in the new equation the intrinsic shielding capabilities of the satellite equipment are considered explicitly.

The BLE has been developed for application to configurations consisting of a Whipple shield or a honeycomb sandwich panel placed in front of a backwall. It considers explicitly the thickness, material and spacing of each of the three involved plates. The backwall represents the cover plate or the external wall of spacecraft equipment that is placed behind the spacecraft's structure wall. The BLE has been experimentally calibrated to the most common spacecraft equipment: fuel and heat pipes, pressure vessels, electronics boxes, harness, and batteries. Further, suitable failure criteria have been defined for each equipment type. The critical projectile masses calculated with the new BLE for satellite equipment placed behind satellite structure walls are considerably larger than the critical projectile masses calculated for the standalone structure wall of the satellite.

## 1. INTRODUCTION

Currently, requirements for spacecraft protection are formulated in terms of the Probability of No Penetration (PNP) of the spacecraft structure wall. This requirement demands that no particle penetrates the structure wall and no material is ejected into the spacecraft interior. Such strict requirement is needed for manned spacecraft, where any penetration may endanger astronauts and any puncture or crack in the structure wall may result in leakage of gas. For satellites however, a PNP requirement for the structure wall may be meaningless, because penetration of the structure will not automatically result in failure of the spacecraft. An additional hole in the structure of a few mm will not result in a structural failure, because the structure walls of satellites are mainly designed against the launch loads. Such PNP requirement overestimates the risk because it does not take into account the intrinsic shielding resistance of the satellite equipment which is offered from e. g. the equipment casing walls, insulations, coatings, etc.

To overcome this shortcoming, under ESA contract 16483 [1] a new ballistic limit equation (SRL equation) has been developed. This equation can be used for the most critical satellite components that are placed behind typical sandwich panel- or Whipple shield structure wall configurations. In contrast to the most frequently used Ballistic Limit Equations for simple double-plate structures (Whipple shields or sandwich panels), e. g. Christiansen [2], Drolshagen and Borge [3], and Reimerdes et al. [4], the SRL (Schäfer–Ryan–Lambert) equation is applicable also to triple plate shield configurations, where the third plate, i.e., the backwall, represents the cover plate or external wall of the equipment that is placed behind the satellite structure wall. The BLE explicitly considers the thickness, material and spacing of each of the three plates.

The SRL BLE has been calibrated with experimental results obtained from hypervelocity impact tests on satellite equipment that was placed behind typical satellite structure walls. The considered equipment were fuel and heat pipes, pressure vessels, electronics boxes, harness, and batteries, all representative of real satellite equipment. To reflect the actual configurations used onboard the spacecraft in a reasonably realistic way, the equipment was placed at defined spacing behind (a) sandwich panels with aluminium honeycomb core and MLI (typical for satellites), (b) standalone MLI (typical for satellites), or (c) single bumper plates or double bumper plates (typical for manned spacecraft). The resulting test configurations were:

- fuel pipes placed behind (a) Al H/C SP structure walls, with MLI, and (b) thin bumper plates

*Proc. '5th European Conference on Space Debris', Darmstadt, Germany 30 March – 2 April 2009, (ESA SP-672, July 2009)*

- heat pipes placed behind Al H/C SP structure walls, with MLI, and (b) heat pipes integrated in sandwich panels
- carbon-fibre overwrapped Al vessels placed behind (a) Al H/C SP structure walls, with MLI, and (b) double plate bumpers
- battery cells placed behind Al H/C SP structure walls, with MLI
- e-boxes placed behind (a) Al H/C SP structure walls, with MLI, and (b) standalone MLI, and
- harnesses placed behind (a) Al H/C SP structure walls, with MLI, and (b) standalone MLI

The test campaign comprised 89 hypervelocity impact tests on operating equipment in configurations representative for satellites, cf. [1], [6], [7], with impact velocities ranging between 2.26 km/s and 7.79 km/s, and projectile sizes of 1.1 mm to 7.0 mm. The vast majority of the impact tests were conducted at perpendicular incidence on the targets. The objective of the impact test campaign was to increase the projectile diameter and/or the impact velocity until failure (Table 1) of the equipment occurred. More details on the impact test campaign can be found e. g. in [9].

## 2. SRL BALLISTIC LIMIT EQUATION

One important requirement for the new ballistic limit equation was to be capable of considering explicitly the thickness, material, and spacing of each of three plates to allow covering the configurations listed in Chapter 1. The first and the second plates represent the spacecraft's structure wall (e.g. honeycomb sandwich panel of a satellite, or bumper and primary structure of a manned spacecraft), the third plate represents the front wall or cover plate of the equipment under consideration (Figure 1).

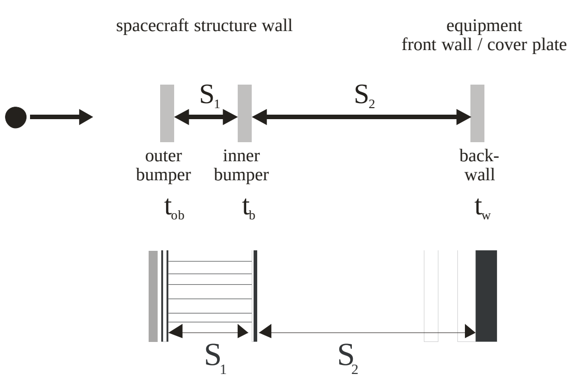


*Figure 1. Baseline geometric configuration for the SRL ballistic limit equation*

The SRL BLE uses a similar notation to the one introduced by ESA for Whipple shields. ESA [3] defines two coefficients, $K_{3S}$ and $K_{3D}$, for adjusting the equation to experimental data. For $K_{3S} = 1$ and $K_{3D} = 0.16$, this equation is the same as the Christiansen BLE [2], except that [2] defines a limiting angle, above which $d_c$ remains constant, while [3] does not have a limit angle criterion. The SRL equation converges to the Whipple shield equation in the limiting cases of $t_w \rightarrow 0$ or $S_2 \rightarrow 0$. The relevant failure modes of the equipment for the SRL equation are listed in Table 1.

*Table 1. Equipment failure modes relevant for SRL BLE*

| equipment type | equipment failure mode* | relevant failure mode for BLE | comment |
|---|---|---|---|
| fuel pipes | leakage of liquid | presence of a crack or hole in pipe wall | Ref. [6] |
| heat pipes | leakage of gas | presence of a crack or hole in pipe wall | Ref. [6] |
| pressure vessels/ tanks | leakage of gas/liquid | presence of a crack or hole in the wall | Refs. [6] and [8] |
| electronics boxes | temporary perturbation of box function | spall detachment from cover plate | Ref. [7] |
| harness | temporary perturbations on signals/ supply voltage | penetration of cable insulation | Ref. [10] |
| batteries (NiCd) | electrical discharge | penetration of battery casing | |

* other failure modes are possible. The indicated ones cover the least severe failure modes only

### 2.1 The SRL equation

The SRL ballistic limit equation is shown in Eqn. (1)-(3). Eqn. (1) shows the critical projectile diameter as a function of impact velocity in the ballistic velocity regime ($v_n \leq v_{t1,n}$), where the projectile does not fragment. With respect to the equations given in [2] and [3], the power of $\alpha$ has been added to the wall thickness of the equipment cover plate $t_w$. Further, a term taking care of the protection enhancement offered by the MLI ($K_{MLI} \cdot t_{eq,MLI}$) has been added.

$$d_c(v) = \left[ \frac{\frac{(t_w^{\alpha} + t_b)}{K_{3S}} \cdot \left(\frac{\sigma_{y,ksi}}{40}\right)^{1/2} + t_{ob} + K_{MLI} \cdot t_{eq,MLI}}{0.6 \cdot (\cos\theta)^{\delta} \cdot \rho_p^{1/2} \cdot v^{2/3}} \right]^{18/19} \qquad (1)$$

where

$$t_{eq,MLI} = \frac{\rho_{AD,MLI}}{\rho_{ob}}$$

In the shatter velocity regime, a linear extrapolation is made between the ballistic (Eqn. (1)) and the hypervelocity regime (Eqn. (3), below). The following equation describes the critical projectile diameter for failure of rear wall, $d_c$, in the shatter velocity regime ($v_{t1,n} < v_n < v_{t2,n}$):

$$d_c(v) = d_c(v_{t1}) + \frac{d_c(v_{t2}) - d_c(v_{t1})}{v_{t2} - v_{t1}} \cdot (v - v_{t1)} \qquad (2)$$

In the equation for the critical projectile diameter in the hypervelocity regime ($v_n \geq v_{t2,n}$), Eqn. (3), compared to [2] and [3], a term $K_{S2} \cdot S_2^{\beta} \cdot t_w^{\gamma} \cdot \cos\theta^{\varepsilon}$ has been added to explicitly consider the equipment. $S_2$ is the stand-off between the rear side of the inner bumper and the equipment front/cover plate. $t_w$ is the equipment cover plate thickness, and $\theta$ the impact angle of the projectile on the target surface. The additional cosine-term introduced in this part of the equation was necessary to account for the experimentally observed tremendous increase of critical projectile diameters in the hypervelocity range at oblique impacts. The data obtained also suggest that stand-off $S_2$ contributes significantly to the enhancement of the protection capability at hypervelocity. The exponents of $S_2$, $t_w$, $\cos\theta$ have to be fit to the experimental data. Fit factor $K_{S2}$ is required to balance the term $S_2^{\beta} \cdot t_w^{\gamma} \cdot \cos\theta^{\varepsilon}$ as all fit parameters $K_{S2}$, $\beta$, $\gamma$, and $\varepsilon$ are inter-related. The sum term $t_b + K_{tw} \cdot t_w$ represents an effective thickness of inner bumper and equipment cover plate ("effective" because of the $K_w$-term). Its significance becomes obvious when considering a case where the equipment is mounted directly on the inner bumper of the structure wall ($S_2 = 0$). This case essentially corresponds to a Whipple shield with an outer bumper and a rear wall constituted by the inner bumper plus the equipment cover plate.

$$d_c(v) = \frac{1.155 \cdot \left( \frac{\sigma_{y,ksi}}{70} \right)^{1/3}}{K_{3D}^{2/3} \cdot \rho_p^{1/3} \cdot \rho_{ob}^{1/9} \cdot v^{2/3} \cdot \cos\theta^{\delta}} \cdot \qquad (3)$$

$$\left[ S_1^{1/3} \cdot \left( t_b + K_{tw} \cdot t_w \right)^{2/3} + K_{S2} \cdot S_2^{\beta} \cdot t_w^{\gamma} \cdot (\cos\theta)^{-\varepsilon} \right]$$

To apply this equation for the calculation of a ballistic limit curve (BLC) of a standalone sandwich panel, $t_w$ and $S_2$ are set to zero. The equation then essentially reduces to the ESA triple wall equation [3] or the Whipple shield equation [2], respectively. To apply it for the case of, e.g., an e-box attached directly to a honeycomb sandwich panel structure wall, $S_2$ has to be set equal to zero. Equation (3) describes the critical projectile diameter for failure of the rear wall, $d_c$, in the hypervelocity regime ($v_n \geq v_{t2,n}$).

## 2.2 Application notes for the SRL equation

To allow completely different structure and equipment types to be considered by the SRL equation, a number of application notes specific to each structure and equipment type have to be defined.

**Application notes for structure walls**

- (S1) MLI with stand-off to equipment > 0: In case standalone MLI is used as the structure wall, the SRL equation essentially is applied as Whipple shield equation. $S_2$ is set to zero and $S_1$ corresponds to the inner spacing between the MLI and the equipment cover plate. $t_{ob}$ shall be set to zero. The MLI structure wall is explicitly considered in the BLE (in the ballistic velocity regime) as $t_{eq,MLI}$ where $t_{eq,MLI}$ is calculated from the MLI areal mass divided by the (volumetric) density of aluminium (2.7 g/cm$^3$) $t_{eq,MLI} = \rho_{AD,MLI}/\rho_{Al}$. For $t_b$, the thickness of the casing wall shall be inserted. For the transition velocities $v_{t1,n}$ and $v_{t2,n}$, 4 km/s and 10 km/s, respectively, shall be used.
- (S2) MLI placed directly on top of equipment: The equation for the critical diameter in the ballistic velocity regime is applied to the whole velocity regime $v_n > 0$. $t_{ob}$ and $t_w$ are set to zero. $t_{eq,MLI}$ is calculated from the MLI areal mass divided by the (volumetric) density of aluminium (2.7 g/cm$^3$) $t_{eq,MLI} = \rho_{AD,MLI}/\rho_{Al}$. This equation effectively corresponds to the Cour-Palais thin wall equation.
- (S3) Standalone equipment cover: This configuration corresponds to direct impacts on unshielded equipment, i.e. impacts on thin plates. Same procedure as for MLI, except that $t_{eq,MLI}$ is set to zero.
- (S4) Single wall shielding: With equipment placed behind a single wall shield, this configuration corresponds to a Whipple shield. Insert the wall thickness of the single wall bumper for $t_{ob}$. Set $t_w$ and $S_2$ equal to zero.
- (S5) Honeycomb sandwich panels: The honeycomb core of a honeycomb sandwich panel is omitted; it shall be replaced by void. The thickness of the honeycomb is the $S_1$ spacing. $S_2$ is the closest spacing between the second bumper and the equipment surface (in normal direction to the plane of the second bumper plate). MLI placed on top of the honeycomb sandwich panel is considered explicitly in the BLE (in the ballistic velocity regime) as $t_{eq,MLI}$ where $t_{eq,MLI}$ is calculated from the MLI areal mass divided by the (volumetric) density of the aluminium alloy used for the outer face-sheet.
- (S6) Double wall shielding: The outer bumper with thickness $t_{ob}$ corresponds to the first bumper of the double wall shield. The inner bumper with thickness $t_b$ corresponds to the second bumper of the double bumper shield. $S_1$ is the inner spacing between first and second bumper, $S_2$ is the closest spacing between the second bumper and the equipment surface (in normal direction

to the plane of the second bumper plate). For $\sigma_{y,ksi}$, the yield stress of the equipment cover wall shall be used. MLI placed on top of the outer bumper is considered explicitly in the BLE (in the ballistic velocity regime) as $t_{eq,MLI}$ where $t_{eq,MLI}$ is calculated from the MLI areal mass divided by the (volumetric) density of the aluminium alloy used for the outer bumper.

**Application notes for equipment**

- (E1) Application to fuel pipes: Equipment placed behind structure walls (S1) to (S4): For $t_b$, use the value of the pipe's wall thickness. If the pipe material is other than aluminium, use for $t_b$ the value as obtained from the equal areal density approach with the density of aluminium for normalization ($t_b = t_{pipe} \cdot \rho_{pipe}/\rho_{Al}$). For the yield stress $\sigma_{y.ksi}$, use the yield stress of the actual pipe material. Equipment placed behind structure walls (S5) to (S6): For $t_w$, use the value of the pipe's wall thickness. If the pipe material is other than aluminium, use for $t_w$ the value as obtained from the equal areal density approach with the density of aluminium for normalization ($t_w = t_{pipe} \cdot \rho_{pipe}/\rho_{Al}$). For the yield stress $\sigma_{y.ksi}$, use the yield stress of the actual pipe material.
- (E2) Application to standalone heat pipes: Equipment placed behind structure walls (S1) to (S4): For heat pipes, two wall thicknesses are supplied: minimum and maximum wall thickness (Figure 2). For the SRL equation, use the maximum wall thickness for $t_b$; if the heat pipe material is other than aluminium, use for $t_b$ the value as obtained from the equal areal density approach ($t_b = t_{pipe} \cdot \rho_{pipe}/\rho_{Al}$). Set $t_w$ and $S_2$ equal to zero. For the yield stress $\sigma_{y.ksi}$, use the yield stress of the actual heat pipe material. Equipment placed behind structure walls (S5) to (S6): For heat pipes, two wall thicknesses are supplied: minimum and maximum wall thickness (Figure 2). For the SRL equation, use the maximum wall thickness for $t_w$. If the heat pipe material is other than aluminium, use for $t_w$ the value as obtained from the equal areal density approach described above ($t_w = t_{pipe} \cdot \rho_{pipe}/\rho_{Al}$). For the yield stress $\sigma_{y.ksi}$, use the yield stress of the actual heat pipe material.

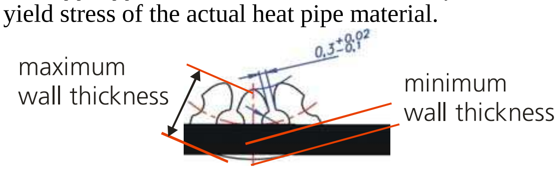


*Figure 2. This figure shows a 1/8-section of a heat pipe in cross-section. The definition of the minimum/ maximum heat pipe wall thickness is shown.*

- (E3) Application to integrated heat pipes in sandwich panel structures: Insert the wall thickness of the sandwich panel's front face-sheet including additional walls (*Figure 3*) for $t_{ob}$. $t_w$ and $S_2$ are set equal to zero. For heat pipes, two wall thicknesses are supplied: minimum and maximum wall thickness (Fig. 5): For the calculations, use the maximum wall thickness for $t_b$. If the heat pipe material is other than aluminium, use for $t_b$ the value as obtained from the equal areal density approach ($t_b = t_{pipe} \cdot \rho_{pipe}/\rho_{Al}$). For bumper density $\rho_b$, use the density of the Al alloy; for the yield stress $\sigma_{y,ksi}$, use the yield stress of the actual heat pipe material.
- (E4) Application to carbon-fibre wrapped vessels: Equipment placed behind structure walls (S5) to (S6): For $t_w$, use the wall thickness of the carbon-fibre wrapped vessel. $t_w$ is calculated according to the following equation:

$$t_w = t_{w,Al} + K_{CFRP} \cdot \left(t_{w,CFRP}\right)^{1/3} \cdot \frac{\rho_{CFRP}}{\rho_{Al}} \qquad (4)$$

where $K_{CFRP}$ is the adjustment factor for CFRP, $t_{w,Al}$ is the thickness of the Al liner of the carbon-fibre wrapped vessel [cm], $t_{w,CFRP}$ is the thickness of the CFRP layer of the carbon-fibre wrapped vessel [cm], $\rho_{Al}$ is the density of the reference aluminium (2.7 g/cm$^3$), and $\rho_{CFRP}$ is the density of the CFRP [g/cm$^3$]. For the yield stress $\sigma_{y.ksi}$, the yield stress of the vessel's liner material shall be used.

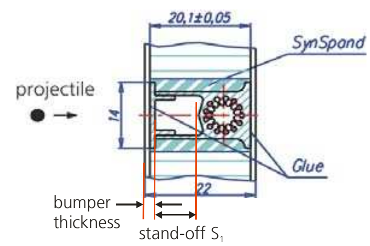


*Figure 3. Definition of bumper thickness and stand-off for integrated heat pipes.*

- (E5) Application to e-boxes placed behind structure walls: Equipment placed behind structure walls (S1) to (S4): For $t_b$, use the value of the e-box casing wall thickness. If the e-box casing wall material is other than aluminium, use for $t_b$ the value as obtained from the equal areal density approach with the density of aluminium for normalization ($t_b = t_{casing} \cdot \rho_{casing}/\rho_{Al}$). For the yield stress $\sigma_{y.ksi}$, use the yield stress of the actual casing wall material. Equipment placed behind structure walls (S5) to (S6): For $t_w$, use the value of the e-box casing wall thickness. If the casing wall material is other than aluminium, use for $t_w$ the value as obtained from the equal areal density approach with the density of aluminium for normalization ($t_b = t_{casing} \cdot \rho_{casing}/\rho_{Al}$). For the yield stress $\sigma_{y.ksi}$ use the yield stress of the actual casing wall material.
- (E6) Application to battery cells placed behind structure walls: Equipment placed behind structure walls (S1)- to (S4): For $t_b$, use the value of the thickness of the battery cell wall (casing). If the material of the battery cell wall is other than aluminium, use for $t_b$ the

value as obtained from the equal areal density approach with the density of aluminium for normalization ($t_b = t_{casing} \cdot \rho_{casing}/\rho_{Al}$). For the yield stress $\sigma_{y.ksi}$, use the yield stress of the actual casing wall material. Equipment placed behind structure walls (S5) to (S6): For $t_w$, use the value of the thickness of the battery cell wall (casing). If the material of the battery cell wall is other than aluminium, use for $t_w$ the value as obtained from the equal areal density approach with the density of aluminium for normalization ($t_b = t_{casing} \cdot \rho_{casing}/\rho_{Al}$). For the yield stress $\sigma_{y.ksi}$, use the yield stress of the actual casing wall material.

- (E7) Application to cables placed behind structure walls: Equipment placed behind structure walls (S2), (S5): From the cable geometry and the materials of the cable components, an effective Al wall thickness is calculated, to be applied in the SRL ballistic limit equation for $t_w$. Correspondingly, failure of the respective cables is assumed when the effective Al wall fails, i.e., when spall detachment occurs. Hence, for the yield stress $\sigma_{y.ksi}$, the yield stress of the aluminium shall be used. This approach is a purely engineering one, not reflecting the actual penetration behaviour of fragments into cables. $t_w$ is calculated according to the following equation:

$$t_w = K_{cable} \cdot \left[ \sum_i^{N_{insul}} \left( t_{insul,i} \cdot \frac{\rho_{insul,i}}{\rho_{Al}} \right) + \sum_j^{N_c} \left( t_{c,j} \cdot \frac{\rho_{c,j}}{\rho_{Al}} \right) \right] \quad (5)$$

where $K_{cable}$ is the adjustment factor for cables, $N_{insul}$ is the total number of insulation layers, $N_c$ is the total number of conductor or metallic shielding layer of the cable, $t_{insul,i}$ is the thickness of i-th insulation layer of the cable [cm], $t_{c,j}$ is the thickness of j-th conductor or metallic shielding layer of the cable [cm], $\rho_{Al}$ is the density of reference Al (2.7 g/cm$^3$), $\rho_{insul,i}$ is the density of i-th insulation layer of the cable [g/cm$^3$], and $\rho_{c,j}$ is the density of j-th conductor or metallic shielding layer of the cable [g/cm$^3$].

**Fit coefficients**

Several parameters in the SRL ballistic limit equation need to be fit to the experimental data. These are general fit parameters that are applied to all equipment types, and equipment specific parameters that need to be fit separately for any equipment type. The general fit parameters are $K_{3S} = 1.40$, $K_{3D} = 0.4$, $K_{MLI} = 3.0$, $K_{S2} = 0.1$, $K_{tw} = 1.5$, $\alpha = 1/2$, $\beta = 2/3$, $\gamma = 1/3$, $\delta = 4/3$ for ($\theta \leq 45°$ and $\theta \geq 65°$) and $\delta = 5/4$ for ($45° < \theta < 65°$), $\varepsilon = 8/3$ for ($\theta \leq 45°$ and $\theta \geq 65°$) and $\varepsilon = 10/4$ for ($45° < \theta < 65°$). The specific fit parameters of the SRL BLE for each equipment/structure type are $v_{t1,n} = 3$ km/s and $v_{t2,n} = 7$ km/s for the following structure walls: Al H/C SP / Al bumper / MLI+Al H/C SP / MLI+Al bumper, $v_{t1,n} = 4$ km/s and $v_{t2,n} = 10$ km/s for standalone MLI as structure wall, $K_{CFRP} = 0.75$ for carbon-fibre wrapped vessels, and $K_{cable} = 0.35$ for cables.

For the fitting of the various coefficients of the SRL BLE, a large number of parametric experimental data is required. In the underlying project [1], only a limited set of test configurations and test data were available, with most of the impact tests having been performed at perpendicular impact, leaving considerable gaps in the validation of the equation especially at oblique impacts. To make sure that all of its coefficients were fitted simultaneously against the experimental data, the SRL BLE became a rather conservative ballistic limit equation.

## 3. BALLISTIC LIMIT CURVES BASED ON SRL EQUATION

For illustration of the SRL ballistic limit equation, in this chapter, ballistic limit curves (BLC) for high-pressure vessels and electronics boxes are plotted against the corresponding experimental results.

### 3.1 High-pressure vessels

The experimental data obtained in hypervelocity impact tests on CFRP/Al high-pressure vessels placed behind the MLI/MetOp Sandwich Panel and the corresponding ballistic limit curves are plotted in Figure 4. As a failure criterion for gas-filled high-pressure vessels, pressure tightness was selected.

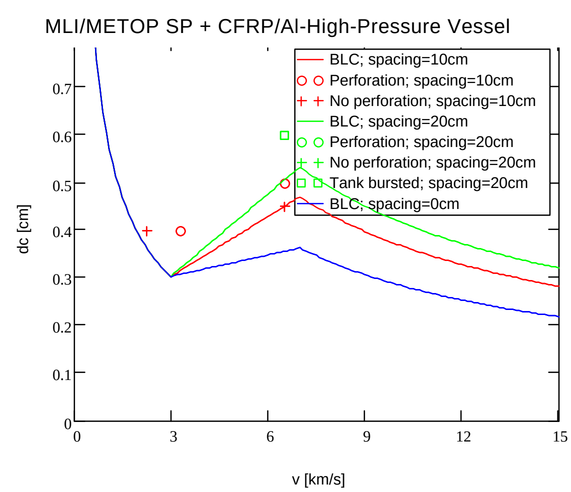


*Figure 4. BLC and experimental results for impact tests on carbon-fibre wrapped pressure vessels with Al liners, with a METOP H/C SP structure wall with MLI placed at a stand-off of 100 mm and 200 mm (and 0 mm) from the vessel surface. 0° impact angle.*

The values used in the SRL equation are: $t_{ob} = 0.041$ cm, $t_b = 0.041$ cm, $t_w = t_{Al} + K_{CFRP} \cdot \rho_{CFRP} \cdot (t_{CFRP})^{1/3} / \rho_{Al} = 0.472$ cm, $R_{p0.2} = 260$ MPa, $\rho_p = 2.7$ g/cm$^3$, $\rho_{ob} = 2.7$ g/cm$^3$, $\rho_b = 2.7$ g/cm$^3$, $m_{a,MLI} = 0.0447$ g/cm$^2$, $\theta = 0°$, $S_1 = 3.5$ cm, $S_2 = 20$ / 10 / 0 cm, bumper material: Al. At 100 mm stand-off between tube/vessel wall and sandwich panel, the experimental results (perforation/no perforation of the vessel wall) are fitted well to the SRL equation. At 200 mm stand-off, the fit is slightly conservative in the lower shatter velocity range.

### 3.2 E-boxes

In Figure 5, some of the results obtained from hypervelocity impact tests on e-boxes shielded with MLI/MetOp H/C SP structure are plotted against the corresponding ballistic limit curve, at 0° and 45°.

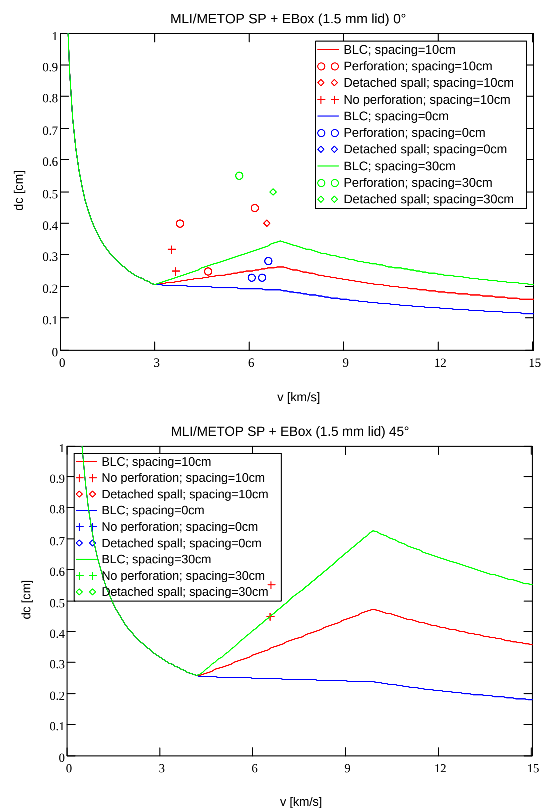


*Figure 5. BLC and experimental results for impact tests on e-box with 1.5 mm thick Al lid, with a METOP H/C SP structure wall with MLI placed at a stand-off of 100 mm and 300 mm (and 0 mm) from the lid's surface. Top: 0° impact angle. Bottom: 45° impact angle.*

The failure criteria were "perforation", "spall detachment" and "no perforation" of the e-box lid. As is known from the hypervelocity impact tests [7], failure criterion "spall detachment" marks the onset of perturbations during operation. The values used in the SRL equation are: $t_{ob} = 0.041$ cm, $t_b = 0.041$ cm, $t_w = 0.15$ cm, $R_{p0.2} = 250$ MPa, $\rho_p = 2.7$ g/cm$^3$, $\rho_{ob} = 2.7$ g/cm$^3$, $\rho_b = 2.7$ g/cm$^3$, $m_{a,MLI} = 0.0447$ g/cm$^2$, $\theta = 0°$ / 45°, $S_1 = 3.5$ cm, $S_2 = 0$ / 10 / 30 cm, bumper material = Al.

## 4. BENEFIT GAINED FROM CONSIDERING THE EQUIPMENT'S INHERENT SHIELDING CAPABILITY

In Figure 6, the SRL BLC has been plotted for the MetOp-H/C SP alone and the MetOp- H/C SP plus e-box configuration. The e-box has a 1.5 mm thick lid. The stand-off between rear face-sheet of the sandwich panel and the equipment front wall is 100 mm. In the case of the e-box with the 1.5 mm thick lid, at 7 km/s, the predicted critical diameter for spall detachment on the rear side of the lid amounts to ca. 2.5 mm while for the standalone MLI+MetOp sandwich panel the predicted critical diameter is on the order of 0.7 mm. The difference in mass between the two critical projectile diameters is a factor of approximately 45. Thus, when considering the intrinsic shielding capabilities of the e-box lid instead of assuming that the e-box fails if the satellite structure wall placed in front of it is perforated, impact of much larger projectile masses can be considered "safe" for the function of the equipment. From this assessment, it can be concluded that the risk of equipment failure is currently overestimated if it is assumed that the equipment fails as soon as the structure wall in front of it is perforated.

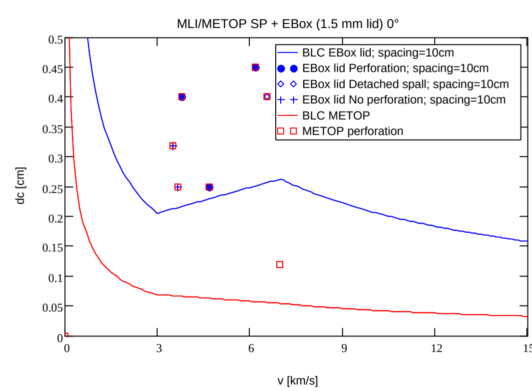


*Figure 6. BLC for a standalone MLI+MetOp sandwich panel and an e-box with a 1.5 mm thick lid placed at a 100 mm stand-off to the MLI+MetOp structure wall. Normal projectile incidence (0°).*

## 5. CONCLUSIONS

A new ballistic limit equation was developed for satellite equipment placed behind satellite structure walls. It was fitted to experimental results from hypervelocity impacts on satellite equipment. This ballistic limit equation considers directly the inherent shielding capabilities of the satellite equipment.

The new equation was applied to show that if the inherent protection capability of satellite equipment against hypervelocity impacts is explicitly considered in a ballistic limit equation, the critical projectile diameters for failure of the equipment are raised considerably compared to the case where equipment is assumed to fail as soon as the structure wall that protects it is perforated. In the example give, in terms of critical projectile mass, the benefit gained can amount up to two orders of magnitude.

## 6. REFERENCES


[1] Schäfer, F., Putzar, R., Lambert, M. (2008). Vulnerability of Satellite Equipment to Hypervelocity Impacts, IAC-08.A6.3.2, Proc. 59th International Astronautical Congress, Sept. 29 - Oct. 3, 2008, Glasgow, Scotland

[2] Christiansen, E. L. (1993). Design and Performance Equations for Advanced Meteoroid and Debris Shields. *Int. J. Impact Engng.* 14, 145-156.

[3] Drolshagen G, Borge J. (1992). ESABASE/DEBRIS. Meteoroid/Debris Impact Analysis Technical Description, *Issue 1 for ESABASE version 90.1*.

[4] Reimerdes, H. G., Stecher, K. H., Lambert, M. (1993). Ballistic Limit Equations for the Columbus Double Bumper Shield Concept. *Proc. First European Conference on Space Debris.* ESA SD-01.

[5] Christiansen, E. L., Kerr, J. (1993). Mesh Double-Bumper Shield: A Low-Weight Alternative for Spacecraft Meteoroid and Orbital Debris Protection, *Int. J. Impact Engng.* 14, 169-180.

[6] Putzar, R., Schäfer, F., Romberg, O., Lambert, M. (2005). Vulnerability of Shielded Fuel Pipes and Heat Pipes to Hypervelocity Impacts. *Proc. 4th European Conference on Space Debris*, ESA SP-587; ISBN 92-9092-898-0.

[7] Putzar, R., Schäfer, F., Stokes, H., Chant, R., Lambert M. (2005). Vulnerability of Spacecraft Electronic Boxes to Hypervelocity Impacts. *Proc. 56th International Astronautical Congress*.

[8] Palmieri, D., Schäfer, F., Hiermaier, S., and Lambert, M. (2001). Numerical simulation of non-perforating impacts on shielded gas-filled pressure vessel. *International Journal of Impact Engineering* 26, 591-602.

[9] Schäfer, F. K. et al. (2008), Ballistic limit equation for equipment placed behind satellite structure walls, International, *Journal of Impact Engineering*, doi:10.1016/j.ijimpeng.2008.07.074

[10] Putzar, R., Schäfer, F., Lambert, M. (2008). Vulnerability of spacecraft harnesses to hypervelocity impacts. Int. J. Impact Engng, doi:10.1016/j.ijimpeng.2008.07.067


## 7. NOMENCLATURE

| | |
|---|---|
| BLC | Ballistic Limit Curve |
| BLE | Ballistic Limit Equation |
| H/C SP | Honeycomb Sandwich Panel |
| HVI | Hypervelocity Impact |
| MLI | Multi-Layer-Insulation |
| SRL | Schäfer – Ryan – Lambert |

| | |
|---|---|
| $d_c$ | critical projectile diameter for failure of backwall [cm] |
| $d_p$ | projectile diameter [cm] |
| $K_{3D}$, $K_{3S}$ | ESA triple wall fit factors for the hyper- and ballistic velocity regimes, respectively [-] |
| $K_{CFRP}$, $K_{MLI}$ | adjustment factors for CFRP and for MLI, respectively, in the SRL BLE [-] |
| $K_{S2}$ | adjustment factor for the scaling of stand-off $S_2$ in the hypervelocity regime [-] |
| $K_{tw}$ | adjustment factor for equipment cover plate thickness, $t_w$, in the hypervelocity regime [-] |
| $S_1$, $S_2$ | stand-off between 1st & 2nd, and 2nd & 3rd bumper, where 3rd bumper = backwall [cm] |
| $t_b$ | thickness of the inner/second bumper (in case of a H/C SP: the rear face-sheet) [cm] |
| $t_{eq,MLI}$ | thickness of an aluminium plate having the same surface mass as the MLI [cm] |
| $t_{ob}$ | thickness of the outer bumper (in case of a H/C SP: front face-sheet) [cm] |
| $t_w$ | thickness of equipment cover plate [cm] |
| $t_{w,Al}$, $t_{w,CFRP}$ | thickness of the Al liner, and the CFRP layer, respectively, of the CFRP vessel [cm] |
| $v$, $v_n$ | impact velocity, and its normal component $v_n = v \cdot \cos\theta$, respectively [km/s] |
| $v_{t1}$ | transition velocity for transition between ballistic- and shatter velocity regime [km/s] |
| $v_{t2}$ | transition velocity between shatter- and hypervelocity regime [km/s] |
| $v_{t1,n}$, $v_{t2,n}$ | normal component of $v_{t1,n} = v_{t1} \cdot \cos\theta$, and $v_{t2,n} = v_{t2} \cdot \cos\theta$, respectively [km/s] |
| $\alpha$, $\beta$, $\gamma$, $\delta$, $\varepsilon$ | fit parameter for the SRL BLE [-] |
| $\rho_{AD,MLI}$ | areal mass (surface density) of MLI [g/cm$^2$] |

| | |
|---|---|
| $\rho_{Al}$, $\rho_{CFRP}$ | volumetric density of the reference Al (2.7 $g/cm^3$), and the CFRP, respectively [$g/cm^3$] |
| $\rho_{ob}$, $\rho_p$ | volumetric density of the outer bumper, and the projectile, respectively[$g/cm^3$] |
| $\sigma_{y,ksi}$ | yield stress of the equipment cover plate [ksi] |
| $\theta$ | impact angle (0° corresponds to perpendicular impact on the target surface) [°] |